



Blue-emitting Ir(III) complexes using fluorinated bipyridyl as main ligand and 1,2,4-triazol as ancillary ligand: syntheses, photophysical properties and performances in devices



Peng Sun^{a, b}, Kexiang Wang^{a, b}, Bo Zhao^{a, b}, Tingting Yang^{a, b}, Huixia Xu^{a, b, *}, Yanqin Miao^{a, b}, Hua Wang^{a, b}, Bingshe Xu^{a, b}

^a Key Laboratory of Interface Science and Engineering in Advanced Materials, Ministry of Education, Taiyuan University of Technology, Taiyuan 030024, PR China

^b Shanxi Research Center of Advanced Materials Science and Technology, Taiyuan 030024, PR China

ARTICLE INFO

Article history:

Received 2 August 2016

Received in revised form

24 October 2016

Accepted 2 November 2016

Available online 4 November 2016

Keywords:

Blue-emitting Ir(III) complexes

1,2,4-triazol

Fluorinated bipyridyl

ABSTRACT

The blue-light-emitting Ir(III) complexes using 2-(3-(trifluoromethyl)-1*H*-1,2,4-triazol-5-yl)pyridine and fluorinated 2-phenylpyridine as ligands were synthesized and characterized in details. Their molecular structures were confirmed by ¹H NMR, FT-IR and elemental analyzer. The emission peaks of complex (F_{2,4}ppy)₂Ir(tfmptz) using 2-(2,4-difluorophenyl)pyridine as main ligand are located at 457 and 481 nm. Increasing the number of F atoms leads to a lower the lowest unoccupied molecular orbital energy level. Phosphorescent organic light-emitting devices doped the synthesized Ir(III) complexes into 4,4'-*N,N'*-dicarbazolebiphenyl as emitting layers were fabricated. The based-(F_{3,4,5}ppy)₂Ir(tfmptz) device shows the maximum current efficiency of 9.9 cd/A with the electroluminescent peaks at 471 and 502 nm.

© 2016 Elsevier Ltd. All rights reserved.

1. Introduction

Phosphorescent organic light-emitting devices (PhOLEDs) are considered to be the promising candidates for the next-generation lighting and display applications.^{1–3} Phosphorescent light-emitting materials of heavy metal complex, especially iridium metal, have the excellent performances in PhOLEDs because of the advantages of a theoretical internal quantum efficiency of 100%.^{4,5} However, the blue-emitting phosphorescent complex remains inferior to that of red and green counterparts, such as color purity and luminance efficiency.^{6,7} The well-known blue Ir(III) emitter of bis[2-(4',6'-difluoro)phenylpyridinato-N,C^{2'}]iridium(III)picolinate (Flrpic) exhibits the moderate external quantum efficiency (EQE) of 5.7% with the 1931 Commission Internationale de L'Eclairage coordinates (CIE) coordinates of (0.16, 0.29).^{8,9} But Flrpic cannot be regarded as a true-blue emitter due to its relatively low triplet energy level (*E_T*) of 2.62 eV and sky-blue emission colors with CIE_y > 0.2.¹⁰ Recently, a variety of blue-emitting Ir(III) complexes by changing the

ancillary ligand of picolinate or using functionalized 2-phenylpyridine (ppy) as main ligands in Flrpic have been reported.^{11–13} The former can alter the energy of the excited state by replacing the picolinate with the other ligands, such as tetrakis(1-pyrazolyl)borate (Flr6) with CIE coordinates of (0.16, 0.26),^{14,15} phosphite ligands with CIE coordinates of (0.16, 0.21),¹² and (pyri-din-2-yl)-1*H*-tetrazolate (FlrN4) with CIE coordinates of (0.15, 0.24)¹¹ et al. Meanwhile, The latter can decrease the highest occupied molecular orbital (HOMO) energy level by introducing electron-withdrawing groups such as –OCF₃, –COCF₂CF₂CF₃,¹⁶ cyan,¹⁷ P=O, S=O¹⁸ or nitrogen atom¹⁹ into the 5-position of difluorophenyl ring. Therefore, the fluorinated ppy is an effective way to tune the emission color of Ir(III) complexes. The conversion of C–H bonds in these complexes to C–F bonds may have several benefits, such as reduction of irradiative exciton decay, enhancement of photoluminescence (PL) efficiency, and electron mobility.^{20,21}

In addition, the functionalized 1, 2, 4-triazole is another ligand of choice for giving blue emission in Ir(III) complexes.^{3,22} In this work, we successfully synthesized two blue Ir(III) complexes consisting of main ligands 2-(4', 6'-difluoro)phenylpyridinato-N,C^{2'}(F_{2,4}ppy) [(F_{2,4}ppy)₂Ir(tfmptz)] and 2-(3,4,5-trifluorophenyl)pyridine (F_{3,4,5}ppy) [(F_{3,4,5}ppy)₂Ir(tfmptz)], and ancillary ligand of

* Corresponding author. Key Laboratory of Interface Science and Engineering in Advanced Materials, Ministry of Education, Taiyuan University of Technology, Taiyuan 030024, PR China.

E-mail address: xuhuixia@tyut.edu.cn (H. Xu).

2-(5-(trifluoromethyl)-4H-1,2,4-triazol-3-yl)pyridine. Both Ir(III) complexes were thermally stable and easily sublimed with good yields with the higher E_T than that of Flrpic. The chemical structures of complexes Flrpic, $(F_{2,4}ppy)_2Ir(tfmptz)$ and $(F_{3,4,5}ppy)_2Ir(tfmptz)$ are shown in Scheme 1. The synthesized procedure are shown in Scheme S1 and S2.

1.1. 2-(3, 4, 5-trifluorophenyl)pyridine ($F_{3,4,5}ppy$)

A mixture of 2-bromopyridine (1.6 g, 10 mmol), (3, 4, 5-trifluorophenyl)boronic acid (1.9 g, 12 mmol), tetrakis(triphenylphosphine)palladium(0) ($Pd(PPh_3)_4$) (170 mg, 0.15 mmol), Na_2CO_3 (2 M, 15 mL, 30 mmol) and tetrahydrofuran (THF) (40 mL) was heated to reflux for 24 h under nitrogen atmosphere. After cooling to room temperature, the water (50 mL) was poured into mixture and extracted with CH_2Cl_2 . The organic extracts were washed using water and dried over using anhydrous $MgSO_4$. The crude product was purified with silica gel column chromatography using a 10:1 mixture of petroleum ether and ethyl acetate as the eluent. The white crystals of 2-(3,4,5-trifluorophenyl)pyridine (1.7 g) were obtained. Yield: 81%, 1H NMR (600 MHz, $CDCl_3$, δ): 8.68 (d, 1H, $J = 4.8$ Hz), 7.81–7.75 (m, 1H), 7.70–7.64 (m, 3H), 7.29 (d, 1H, $J = 7.5$ Hz). ^{19}F NMR (377 MHz, $CDCl_3$, δ): -133.94 (d, $J = 20.9$ Hz), -160.01 (t, $J = 20.8$ Hz). FT-IR (KBr, cm^{-1}): 3640, 3146, 1617, 1572, 1531, 1475, 1148, 1416, 1359, 1258, 1202, 1036, 858, 778. Anal. Calcd for $C_{10}H_5F_3N_2$: C, 40.17; N, 29.29; H, 6.69. Found: C, 40.55; N, 28.87; H, 7.13.

1.1.1. 2-(3-(trifluoromethyl)-1H-1,2,4-triazol-5-yl)pyridine (tfmptz)

a. A mixture solution of picolinonitrile (1.0 g, 10 mmol), sodium methoxide (0.05 g, 1 mmol), and methanol (20 mL) was stirred for 10 h at room temperature under nitrogen atmosphere. Then NH_4Cl (0.5 g, 10 mmol) be added and reacted other 20 h at room temperature. The mixture was heated to reflux for 4 h. After cooling to room temperature, the mixture was added a lot of diethyl ether and then filtered. The white crystals of pyridine-2-carboximidamide hydrochloride were obtained.

b. A mixture solution of ethyl trifluoroacetate (2.0 g, 14 mmol), hydrazine hydrate (1.0 g, 21 mmol), and THF (20 mL) was stirred for 12 h at room temperature under nitrogen atmosphere. Then after NaOH (0.5 g, 14 mmol) and pyridine-2-carboximidamide hydrochloride (2.0 g, 15 mmol) were added into the mixture and heated to reflux for 12 h. After cooling to room temperature, the saturated $NaHCO_3$ solution was added and then extracted with ethyl acetate. The organic extract was with water and dried over anhydrous $MgSO_4$. The crude product was subjected to silica gel column chromatography using a 3:1 mixture of petroleum ether and ethyl acetate as the eluent. The white crystals of 2-(3-(trifluoromethyl)-1H-1,2,4-triazol-5-yl)pyridine were obtained. Yield: 82%. 1H NMR (600 MHz, $CDCl_3$, δ): 13.40 (s, 1H), 8.82–8.77 (m, 1H), 8.32 (d, 1H,

$J = 7.9$ Hz), 7.97 (t, 1H, $J = 7.8$ Hz), 7.53 (d, $J = 7.7$ Hz, 1H). FT-IR (KBr, cm^{-1}): 3137, 1606, 1494, 1461, 1428, 1217, 1189, 1009, 765, 714. Anal. Calcd for $C_8H_{16}N_5F_3$: C, 40.17; N, 29.29; H, 6.69. Found: C, 40.55; N, 28.87; H, 7.13.

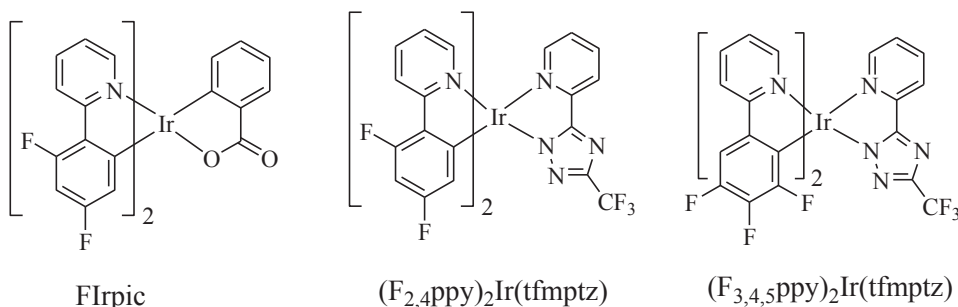
1.2. $(F_{2,4}ppy)_2Ir(tfmptz)$

A mixture solution of 2-(2,4-difluorophenyl)pyridine (0.48 g, 2.5 mmol), $IrCl_3 \cdot 3H_2O$ (0.35 g, 1 mmol), 2-ethoxyethanol (15 ml) and H_2O (5 ml) was refluxed at 120 °C for 24 h under nitrogen atmosphere. After cooling to room temperature, a lot of water was added and then precipitate was filtered, washed by water, ethanol and diethyl ether to obtain the intermediate chloro-bridged dimer $(F_{2,4}ppy)_2Ir(\mu-Cl)_2Ir(F_{2,4}ppy)_2$.

Without further purification, a mixture of the $(F_{2,4}ppy)_2Ir(\mu-Cl)_2Ir(F_{2,4}ppy)_2$ (0.37 g, 0.3 mmol), Na_2CO_3 (0.64 g, 6 mmol), and 2-(3-(trifluoromethyl)-1H-1,2,4-triazol-5-yl)pyridine (64.2 mg, 0.3 mmol) was added into 2-ethoxyethanol (20 ml) and heated to reflux at 140 °C for 24 h under a nitrogen atmosphere, then extracted with CH_2Cl_2 and dried over anhydrous Na_2SO_4 . The crude product was subjected to silica gel column chromatography using a 10:1 mixture of CH_2Cl_2 and ethanol as the eluent. The yellow solid of $(F_{2,4}ppy)_2Ir(tfmptz)$ were obtained. Yield: 40%. 1H NMR (600 MHz, $CDCl_3$, δ): 8.31–8.23 (m, 3H), 7.91 (t, 1H, $J = 7.8$ Hz), 7.74 (d, 3H, $J = 10.2$ Hz), 7.42 (d, 1H, $J = 5.8$ Hz), 7.00 (t, 1H, $J = 6.5$ Hz), 6.90 (t, 1H, $J = 6.5$ Hz), 6.52 (s, 1H), 6.45 (s, 1H), 5.77 (d, 1H, $J = 8.4$ Hz), 5.67 (d, 1H, $J = 8.7$ Hz). ^{19}F NMR (377 MHz, $CDCl_3$, δ): -63.32, -106.66 (d, $J = 10.9$ Hz), -107.26 (d, $J = 10.9$ Hz), -109.29 (d, $J = 11.4$ Hz), -109.91 (d, $J = 11.5$ Hz). FT-IR (in KBr, cm^{-1}): 3616, 3083, 1602, 1478, 1405, 1294, 1243, 1173, 1132, 987, 820, 758. MALDI-TOF: calcd for $IrC_{30}H_{16}N_6F_7$, 785.51; found, 785.84; Anal. Calcd for $IrC_{30}H_{16}N_6F_7$: C, 45.86; N, 10.7; H, 2.03. Found: C, 46.04; N, 10.09; H, 2.31.

1.3. $(F_{3,4,5}ppy)_2Ir(tfmptz)$

The procedure is similar with the synthesis of $(F_{2,4}ppy)_2Ir(tfmptz)$ by using $F_{3,4,5}ppy$ (0.52 g, 2.5 mmol) as main ligand and tfmptz as ancillary ligand. Overall yields: 44%. 1H NMR (600 MHz, $CDCl_3$, δ): 8.26–8.20 (m, 3H), 8.15 (t, 1H, $J = 7.8$ Hz), 8.07 (d, 2H, $J = 36.7$ Hz), 7.90 (t, 2H, $J = 7.8$ Hz), 7.85 (d, 1H, $J = 5.6$ Hz), 7.54 (d, 1H, $J = 5.9$ Hz), 7.50 (d, 1H, $J = 7.3$ Hz), 7.38–7.34 (m, 1H), 7.18 (d, 1H, $J = 7.3$ Hz), 7.11 (d, 1H, $J = 7.4$ Hz). ^{19}F NMR (377 MHz, $CDCl_3$, δ): -63.41, -127.51 (dd, $J = 24.1, 5.2$ Hz), -128.89 (dd, $J = 23.3, 5.1$ Hz), -142.38 (dd, $J = 19.6, 5.3$ Hz), -143.81 (dd, $J = 19.8, 5.2$ Hz), -157.18 (dd, $J = 24.4, 19.3$ Hz), -157.75 (dd, $J = 23.9, 19.6$ Hz). FT-IR (KBr, cm^{-1}): 3670, 3310, 2925, 1610, 1474, 1409, 1350, 1300, 1202, 1140, 1040, 814, 758. MALDI-TOF: calcd for $IrC_{30}H_{14}N_6F_9$, 821.49; found, 821.94; Anal. Calcd for $IrC_{30}H_{14}N_6F_9$: C, 43.85; N, 10.20; H, 1.70. Found: C, 44.52; N, 10.04; H, 1.869. The 1H



Scheme 1. Chemical structures of Flrpic, $(F_{2,4}ppy)_2Ir(tfmptz)$ and $(F_{3,4,5}ppy)_2Ir(tfmptz)$.

NMR, ^{19}F NMR and MS spectra of all compounds are all shown in supporting information.

1.4. General information

The NMR spectra were recorded with a Bruker spectrometer at 600 or 377 MHz (600 for ^1H , 377 MHz for ^{19}F) at ambient temperature. Chemical shifts are given in ppm. Mass spectra were obtained on SHIMADZU matrix-assisted laser desorption/ionization time-of-flight mass spectrometer (MALDI-TOF-MS). C, H, and N microanalysis were carried out with an Elemental Vario EL Elemental analyzer. FT-IR spectra were measured with a Nicolet 7199B spectrometer in KBr pellets in the range of 4000–400 cm^{-1} . UV–vis absorption spectra were measured using Lambda Bio 40. The Photoluminescence (PL) spectra were recorded by HORIBA FluoroMax-4 spectrophotometer. The low-temperature phosphorescence spectra at 77 K in 2-methyltetrahydrofuran (2-MeTHF) and excited-state lifetime in film were measured on an Edinburgh F-980 spectrometer. The absolute quantum yields of the complexes were determined through an absolute method by employing an integrating sphere. Thermogravimetric analysis curves (TGA) were undertaken using a Netzsch TG 209F3 under dry nitrogen atmosphere heating at a rate of 10 $^{\circ}\text{C}/\text{min}$.

Theoretical calculations were performed using the Gaussian 03 package. Geometry optimization was performed on the ground state of each complex by density functional theory (DFT) in B3LYP/6-31G(d) basis sets for N, H, C and LANL2DZ basis sets for Ir atom. The molecular orbital distributions, involving of the highest occupied molecular orbitals (HOMO) and the lowest unoccupied molecular orbitals (LUMO) were analyzed.

Cyclic voltammetry (CV) was measured out in film by drop-coating with chromatographic purity at room temperature using a CHI 660E voltammetry analyzer. The platinum wire is used as working electrode. The platinum electrode is the counter and a calomel electrode is the reference. The scan rate for CV curves is 100 mV s^{-1} . The HOMO levels were calculated according to the equation $E_{\text{HOMO}} = -4.8 - eE_{\text{c}}^{\text{ox}}$, where E_{c}^{ox} was the first oxidation peaks measured from CV curves. On the other hand, the LUMO levels were calculated based on the equation $\text{LUMO} = \text{HOMO} + E_{\text{g}}$, and E_{g} is from the intersection of absorption and emission spectra.

PhOLEDs with area of $3 \times 3 \text{ mm}^2$ were fabricated by vacuum deposition onto indium tin oxide (ITO) glass substrate. ITO glass substrate was cleaned with deionized water, acetone and ethanol in turn. The electroluminescent (EL) spectra and CIE coordinates were measured by PR-655 spectrophotometer. The current density - voltage - luminance (J-V-L) characteristics of PhOLEDs were recorded using Keithley 2400 Source Meter and ST-900M Spot Brightness Meter.

2. Results and discussion

2.1. Synthesis

Both complexes $(\text{F}_{2,4}\text{ppy})_2\text{Ir}(\text{tfmptz})$ and $(\text{F}_{3,4,5}\text{ppy})_2\text{Ir}(\text{tfmptz})$ were synthesized according to the previously reported standard procedures, in which the ligand exchange with corresponding ancillary ligands afforded the titled Ir(III) complexes in Scheme 1. The ligands $\text{F}_{2,4}\text{ppy}$ and $\text{F}_{3,4,5}\text{ppy}$ were reacted with iridium trichloride hydrate ($\text{IrCl}_3 \cdot 3\text{H}_2\text{O}$) to yield the cyclometalated Ir(III) μ -chloride bridged dimer with the quantitative yield. The dimer was converted to the heteroleptic Ir(III) complexes $(\text{F}_{2,4}\text{ppy})_2\text{Ir}(\text{tfmptz})$ and $(\text{F}_{3,4,5}\text{ppy})_2\text{Ir}(\text{tfmptz})$ by replacing the two bridge chlorides with 2-(3-(trifluoromethyl)-1*H*-1,2,4-triazol-5-yl)pyridine. The complexes were confirmed by ^1H NMR, elemental analysis and FT-IR. The photophysical properties were

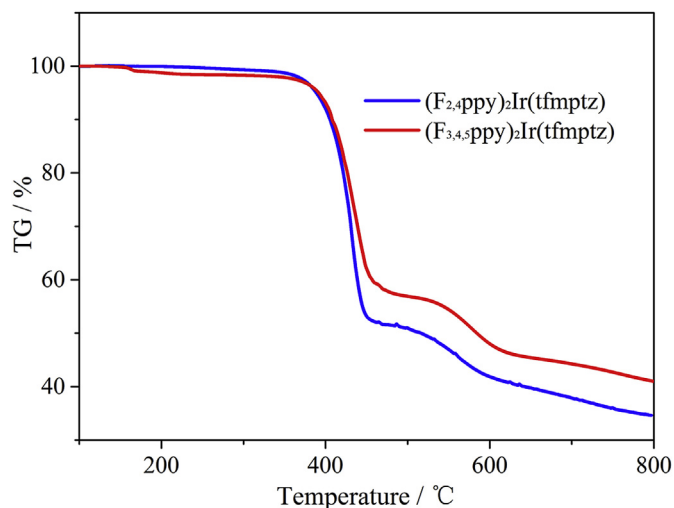


Fig. 1. TGA curves of all title complexes.

characterized by thermal gravimetric analysis (TGA), CV, UV–vis and PL spectroscopy.

2.2. Thermal stability

The thermal properties of complexes were analyzed by TGA and the curves are shown in Fig. 1. The onset of decomposition temperature (T_d , the temperature at which 5% weight loss) was 388 and 391 $^{\circ}\text{C}$ for $(\text{F}_{2,4}\text{ppy})_2\text{Ir}(\text{tfmptz})$, and $(\text{F}_{3,4,5}\text{ppy})_2\text{Ir}(\text{tfmptz})$, respectively. This guaranteed the fast train sublimation with good yield without much residue at higher temperatures.

2.3. Photophysical properties

Fig. 2 shows the steady-state UV–vis absorption and PL spectra of $(\text{F}_{2,4}\text{ppy})_2\text{Ir}(\text{tfmptz})$ and $(\text{F}_{3,4,5}\text{ppy})_2\text{Ir}(\text{tfmptz})$ in CH_2Cl_2 solution and the corresponding spectra data are summarized in Table 1. The absorption spectra at room temperature feature characteristic transition involving strong ligand-centered (LC) spin-allowed π - π^* transition around 253 and 256 nm for $(\text{F}_{2,4}\text{ppy})_2\text{Ir}(\text{tfmptz})$ and $(\text{F}_{3,4,5}\text{ppy})_2\text{Ir}(\text{tfmptz})$, respectively. The singlet metal-to-ligand charge transfer ($^1\text{MLCT}$) transitions are observed in the ranges of 363–384 and 362–382 nm. The calculations indicated that these

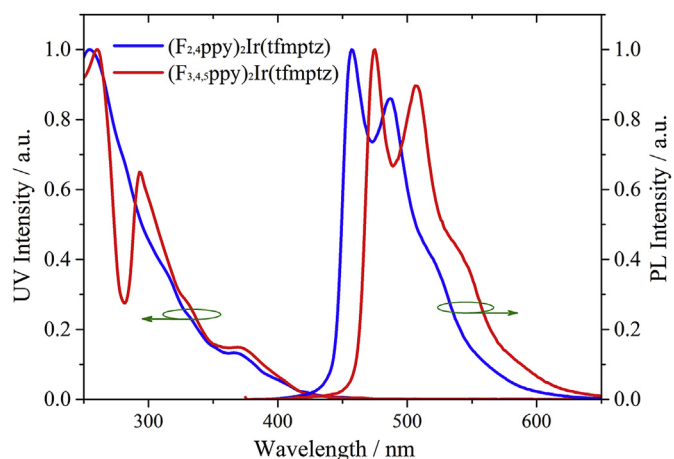


Fig. 2. UV–vis absorption, emission spectra in CH_2Cl_2 solution at room temperature and phosphorescent spectra in 2-MeTHF at 77 K.

Table 1
Photophysical, and electrochemical properties of complexes $(F_{2,4}ppy)_2Ir(tfmptz)$ and $(F_{3,4,5}ppy)_2Ir(tfmptz)$.

Complexes	λ_{abs}^a (nm)	λ_{em}^a (nm)	T_1^b (eV)	T_d ($^{\circ}C$)	HOMO ^c (eV)	E_g^d (eV)	Φ_{PL}^e %	τ^e μs
$(F_{2,4}ppy)_2Ir(tfmptz)$	372, 400	457, 481	2.74	388	−5.51	2.9	20.1	2.48
$(F_{3,4,5}ppy)_2Ir(tfmptz)$	371, 402	469, 502	2.67	391	−5.54	2.8	24.3	3.23

^a Recorded in CH_2Cl_2 solution at room temperature.

^b Triplet level (T_1) calculated based on low-temperature PL spectra at 77 K in 2-MeTHF solution.

^c Measure in film by drop-coating.

^d Measured in the film.

^e Band gap (E_g) was estimated from the intersection of UV–vis and emission spectra.

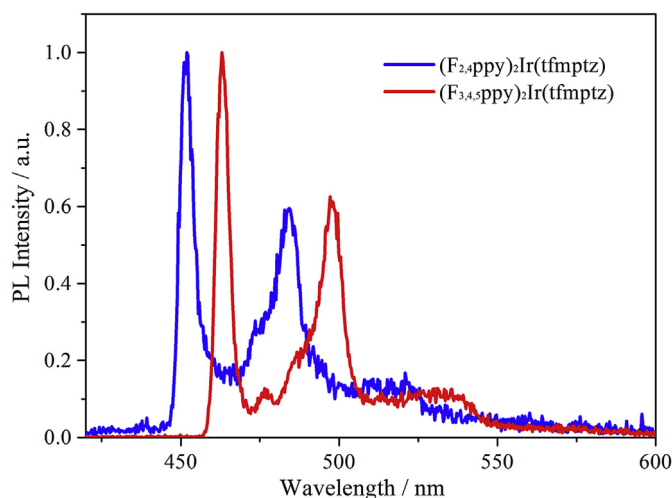


Fig. 3. Phosphorescent spectra in 2-MeTHF at 77 K.

absorptions correspond to the transitions from HOMO-1 to LUMO (89%) with the oscillator strength (f) of 0.0698 and 0.0762. The spin-forbidden MLCT (3MLCT) transition appeared at 400 and 402 nm with the weak absorption, are mainly ascribed to the transition from HOMO to LUMO. The two complexes have very similar absorption, suggesting that the introduction of a fluorine atom at the main ligands did not greatly affect the ground state.

The emission spectra of titled complexes are also displayed in Fig. 2. The vibronic structure of emission bands indicate a large amount of 3LC character, and the excited state is believed to be a mixture of 3LC and 3MLCT .^{23,24} The complex of $(F_{2,4}ppy)_2Ir(tfmptz)$ shows the emission maximum peaks at 457 and 481 nm, and the emission bands of $(F_{3,4,5}ppy)_2Ir(tfmptz)$ appears at 469 nm with a vibronic peak at 502 nm with the higher absolute quantum yields (Φ_{PL}) of 24.3% in film. This result indicates that the fluorine atoms on the main ligand have obvious effects on the excited state of the Ir(III) complexes. The band gaps (E_g) of 2.92 and 2.82 eV were attained by using the intersection of absorption and PL spectra at room temperature in CH_2Cl_2 solution. The excited-state lifetimes (τ) of $(F_{2,4}ppy)_2Ir(tfmptz)$ and $(F_{3,4,5}ppy)_2Ir(tfmptz)$ in film are 2.48

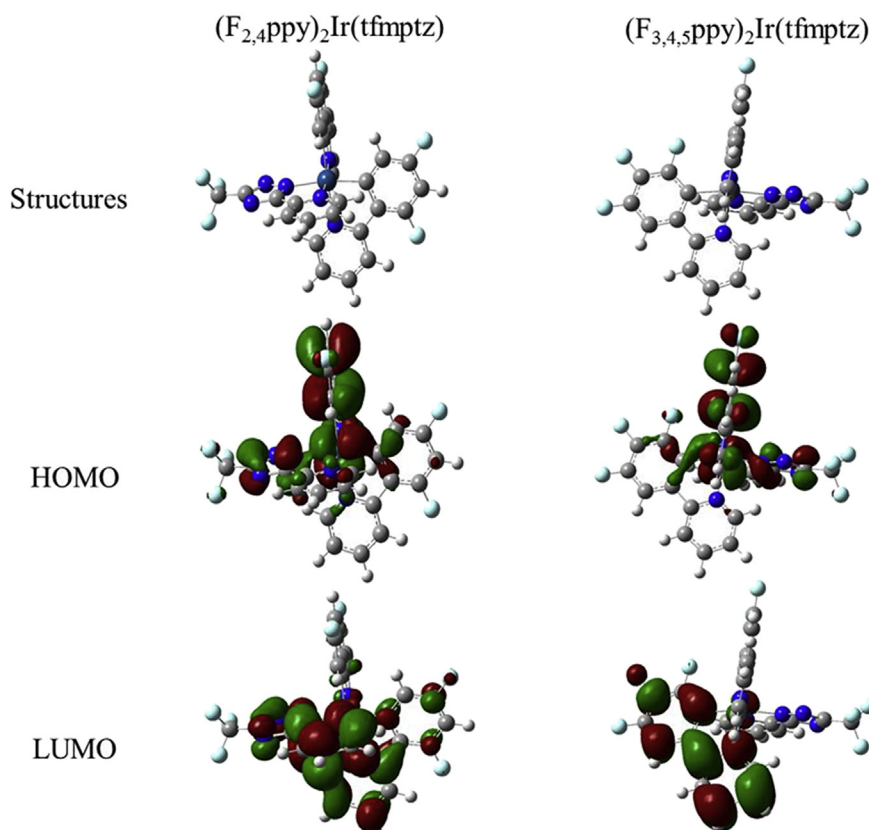


Fig. 4. Optimized molecular structures, HOMO and LUMO of complexes $(F_{2,4}ppy)_2Ir(tfmptz)$ and $(F_{3,4,5}ppy)_2Ir(tfmptz)$.

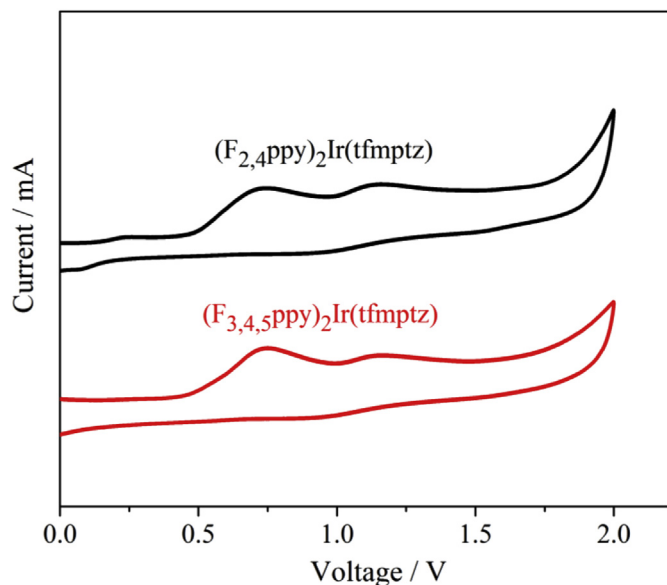


Fig. 5. Cyclic voltammograms of $(F_{2,4}ppy)_2Ir(tfmptz)$ and $(F_{3,4,5}ppy)_2Ir(tfmptz)$.

and 3.23 μs , respectively.

The low-temperature emission spectra in 2-MeTHF at 77 K display the well-resolved vibrational features with blue-shifted by 10 nm with respect to the spectra at ambient temperature (Fig. 3), giving further evidence for the 3MLCT character of the excited state.^{24,25} The triplet energies (E_T) of complexes $(F_{2,4}ppy)_2Ir(tfmptz)$ and $(F_{3,4,5}ppy)_2Ir(tfmptz)$ were estimated to be 2.74 and 2.67 eV. These values are higher than that of Irpic ($E_T = 2.62$ eV)²⁶ owing to the strong σ -donor and weak π -acceptor of ancillary ligand.

To study the effects of the number of F on excited state, density

functional theory (DFT) calculations were employed. The DFT calculations show that the HOMO of $(F_{2,4}ppy)_2Ir(tfmptz)$ is populated on the one of the two $F_{2,4}ppy$ (45.2%), 1,2,4-triazole moieties (4.2%) and d metal orbitals of Ir (50.8%). While the LUMO is mainly localized on the other $F_{2,4}ppy$ moieties (55.9%), mainly localized on the pyridyl fragment, ancillary ligand of tfmptz (42.0%) and Ir orbital (3.2%),²⁷ as shown in Fig. 4. The complexes of $(F_{3,4,5}ppy)_2Ir(tfmptz)$ and $(F_{2,4}ppy)_2Ir(tfmptz)$ have the similar molecular orbitals. The percentage of the Ir atom to HOMO and LUMO are 53.2% and 3.0%.

2.4. Electrochemical properties

To better understand the nature of the electronic structures, cyclic voltammetry (CV) measurements were performed. The electrochemical data were listed in Table 1. The oxidation of

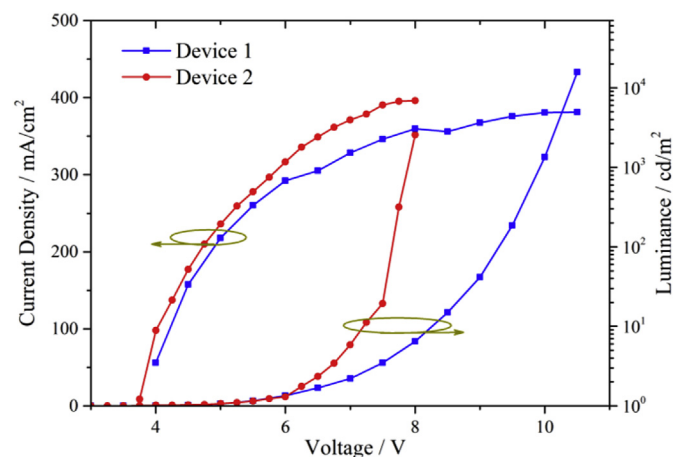


Fig. 7. Current density-voltage-luminance curves of devices.

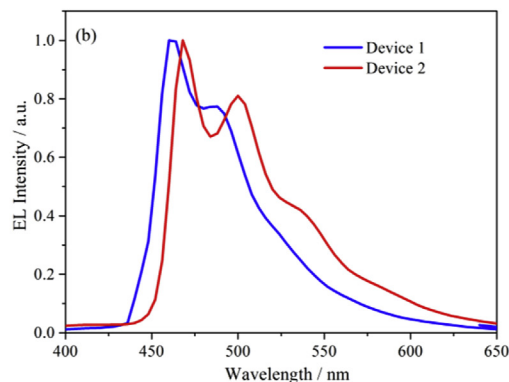
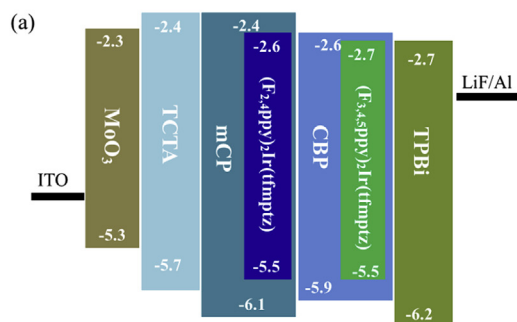


Fig. 6. The energy level diagram (a) and EL spectra (b) of Devices 1 and 2 (mCP: $(F_{2,4}ppy)_2Ir(tfmptz)$ for Device 1; CBP: $(F_{3,4,5}ppy)_2Ir(tfmptz)$ for Device 2).

Table 2

Device performances of devices 1 and 2.

Device	λ_{max}^a (nm)	$V_{turn-on}^b$ (V)	L_{max}^c (cd/m ²)	η_c^d (cd/A)	η_p^e (lm/W)	CIE (x, y)	$\eta_{EQE, max}^f$ (%)
Device 1	460, 490	4.0	4937	5.2	3.0	(0.17, 0.23)	3.0
Device 2	471, 502	3.7	6881	9.9	5.2	(0.21, 0.39)	4.4

^a The maximum peaks at EL spectra.

^b Voltage at a luminance of 1 cd/m².

^c The maximum luminance.

^d The maximum current efficiency.

^e The maximum power efficiency.

^f The maximum external quantum efficiency.

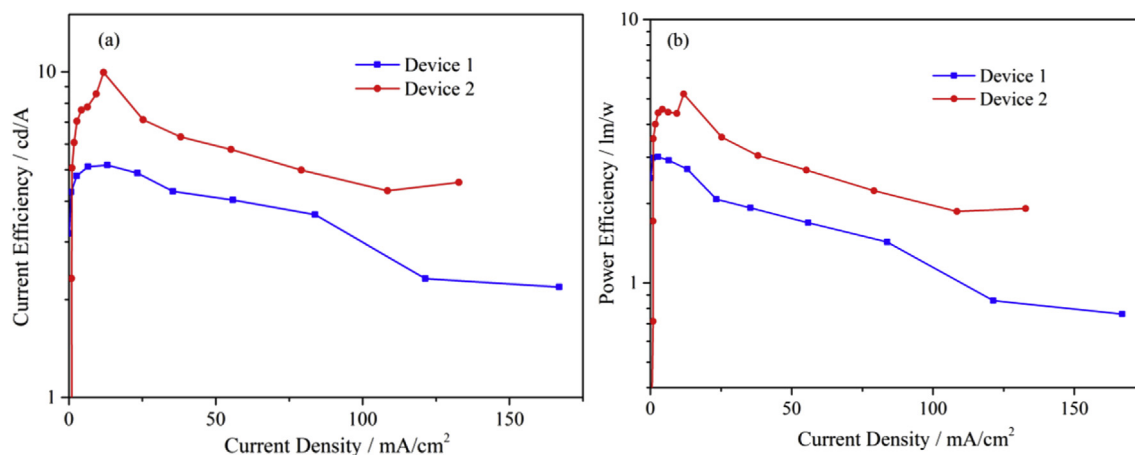


Fig. 8. Current efficiency-current density (a) and Current efficiency-power efficiency (b) curves of PhOLEDs.

complexes $(F_{2,4}ppy)_2Ir(tfmptz)$ and $(F_{3,4,5}ppy)_2Ir(tfmptz)$ are $E_c^{ox} = 0.71$ and 0.74 V, as shown in Fig. 5. The HOMO energy levels were calculated to be -5.51 and -5.54 eV. Therefore, the LUMO energy levels of -2.61 and -2.74 eV were obtained by $LUMO = E_g - HOMO$. While, the calculated HOMO/LUMO energy levels are $-5.71/-1.84$ and $-5.66/-2.02$ eV for $(F_{2,4}ppy)_2Ir(tfmptz)$ and $(F_{3,4,5}ppy)_2Ir(tfmptz)$, respectively. The LUMO energy levels were regulated by introduction of the more electron-withdrawing fluorine atom.

2.5. Performances in PhOLEDs

Based on the properties data in solution, two complexes were applied to construct PhOLEDs. The compound of 1,3-bis(*N*-carbazolyl)benzene (mCP) with T_1 of 2.90 eV was selected as the host in based- $(F_{2,4}ppy)_2Ir(tfmptz)$ device (Device 1). In based- $(F_{3,4,5}ppy)_2Ir(tfmptz)$ device, 4, 4'-*N*, *N'*-dicarbazolebiphenyl (CBP, $T_1 = 2.56$ eV) were employed as host (Device 2). The devices were fabricated by the vacuum sublimation with the structures of ITO/MoO₃ (3 nm)/TCTA (25 nm)/mCP: $(F_{2,4}ppy)_2Ir(tfmptz)$ 4.5 wt% (15 nm)/TPBi (35 nm)/LiF (1 nm)/Al (200 nm) (Device 1) and ITO/NPB (30 nm)/TCTA (10 nm)/CBP: $(F_{3,4,5}ppy)_2Ir(tfmptz)$ 8%wt (30 nm)/TPBi (35 nm)/LiF (1 nm)/Al (200 nm) (Device 2). *N*'-bis(naphthalene)-*N*,*N'*-bis(phenyl)-benzidine (NPB) was used as hole-transport layer; and 1,3,5-tris(2-nhenylbenzimidazolyl)-benzene (TPBi) with $T_1 = 2.6$ eV was used as electron-transport materials. Tris(4-carbazoyl-9-ylphenyl)amine (TCTA) with $T_1 = 2.85$ eV can reduce hole injection barrier. MoO₃ and LiF (lithium fluoride) served as the hole- and electron-injecting layers, respectively. The energy level diagrams of device 1 and 2 are displayed in Fig. 6a. The performances of devices were measured in the air at room temperature.

The EL spectra and representative performance data of Ir(III) complexes are depicted in Fig. 6b and Table 2, respectively. The EL spectra show a dominant emission from the Ir(III) complex without any other residual emission from host or adjacent layers, thus revealing effective energy transfer from the host to Ir dopants. The CIE of Device 1 and 2 calculated from the EL spectra at the voltage of 8 V are (0.17, 0.23) and (0.21, 0.39), respectively. The CIE coordinates of the device incorporating $(F_{2,4}ppy)_2Ir(tfmptz)$ indicate purer and bluer emission than the device doped with $(F_{3,4,5}ppy)_2Ir(tfmptz)$. Additionally, the EL spectra of two devices barely change and CIE values remain almost constant.

The J-V-L characteristics, efficiency-versus-current density curves of two devices are shown in Fig. 7. The Device 1 exhibits a

turn-on voltage at 4.0 V (defined as voltage at a luminance of 1 cd/m²) and a maximum luminance of 4937 cd/m². The peak current and luminescent efficiencies, without any device optimization, are 5.2 cd/A and 3.0 lm/W, respectively, in Fig. 8. Similarly, the Device 2 shows a maximum luminance (L_{max}) of 6881 cd/m² with the maximum current efficiencies (η_c) and maximum power efficiency (η_p) of 9.9 cd/A and 5.5 lm/W, respectively. The maximum external quantum efficiency (η_{EQE}) reached 3% and 4.4% for Devices 1 and 2.

It is difficult to select suitable carrier-injection and transport materials for based- $(F_{2,4}ppy)_2Ir(tfmptz)$ blue PhOLEDs due to the higher T_1 . So the performances of based- $(F_{2,4}ppy)_2Ir(tfmptz)$ devices are inferior to that of the $(F_{3,4,5}ppy)_2Ir(tfmptz)$.

3. Conclusions

In conclusion, two blue-emitting Ir(III) complexes based on 2-(3-(trifluoromethyl)-1*H*-1,2,4-triazol-5-yl)pyridine as ancillary ligand, 2-(3, 4, 5-trifluorophenyl)pyridine ($F_{3,4,5}ppy$) and 2-(2, 4-difluorophenyl)pyridine ($F_{2,4}ppy$) as main ligands have been reported and their photophysical properties have been investigated. A blue emitter of $(F_{2,4}ppy)_2Ir(tfmptz)$ was obtained with the maximum emission peaks at 457 and 481 nm. The conversion of C–F to C–H bonds of 2-position at 2-phenylpyridine results in a red shift of emission. The LUMO is mainly localized on fluorinated 2-phenylpyridine moieties, ancillary ligand with minor contribution of the d Ir(III) orbitals. The $(F_{2,4}ppy)_2Ir(tfmptz)$ -based devices have the superior performances with the current efficiency of 5.2 cd/A.

Acknowledgments

This work was financially supported by the International Science and Technology Cooperation Program of China (2012DFR50460); National Natural Scientific Foundation of China (21071108, 60976018, 61274056, 61205179, 61605138); Natural Science Foundation of Shanxi Province (2015021070); Program for Changjiang Scholar and Innovation Research Team in University (IRT0972); and Shanxi Provincial Key Innovative Research Team in Science and Technology (201513002-10).

Appendix A. Supplementary data

Supplementary data related to this article can be found at <http://dx.doi.org/10.1016/j.tet.2016.11.012>.

References

1. Choy WCH, Chan WK, Yuan Y. *Adv Mater.* 2014;26:5368.
2. Xu H, Chen R, Sun Q, et al. *Chem Soc Rev.* 2014;43:3259.
3. Ho C-L, Wong W-Y. *New J Chem.* 2013;37:1665.
4. Liao J-L, Chi Y, Sie Z-T, et al. *Inorg Chem.* 2015;54:10811.
5. Hwang J, Yook KS, Lee JY, Kim Y-H. *Dyes Pigments.* 2015;121:73.
6. Duan T, Chang T-K, Chi Y, et al. *Dalton Trans.* 2015;44:14613.
7. Lee J, Chen H-F, Batagoda T, et al. *Nat Mater.* 2015;15:92.
8. Holmes RJ, Forrest SR, Tung Y-J, Kwong RC, Brown JJ, Garon S. *Appl Phys Lett.* 2003;82:2422.
9. Tokito S, Iijima T, Suzuri Y, Kita H, Tsuzuki T, Sato F. *Appl Phys Lett.* 2003;83:569.
10. Yang X, Xu X, Zhou G. *J Mater Chem C.* 2015;3:913.
11. Yeh S-J, Wu M-F, Chen C-T, et al. *Adv Mater.* 2005;17:285.
12. Sanner RD, Cherepy NJ, Young Jr VG. *Inorganica Chimica Acta.* 2016;440:165.
13. Takahira Y, Murotani E, Fukuda K, Vohra V, Murata H. *J Fluor Chem.* 2016;181:56.
14. Holmes RJ, D'Andrade BW, Forrest SR, Ren X, Li J, Thompson ME. *Appl Phys Lett.* 2003;83:3818.
15. Zhang B, Liu L, Tan G, et al. *J Mater Chem C.* 2013;1:4933.
16. Lee S, Kim SO, Shin H, et al. *J Am Chem Soc.* 2013;135:14321.
17. Yook KS, Lee JY. *Org Electron.* 2011;12:1711.
18. Fan C, Li YH, Yang CL, Wu HB, Qin JG, Cao Y. *Chem Mater.* 2012;24:4581.
19. Kang Y, Chang YL, Lu JS, et al. *J Mater. Chem C.* 2013;1:441.
20. Wang C-C, Jing Y-M, Li T-Y, et al. *Eur J Inorg Chem.* 2013:5683.
21. Tao S, Lai SL, Wu C, et al. *Org Electron.* 2011;12:2061.
22. Xu QL, Wang CC, Li TY, et al. *Inorg Chem.* 2013;52:4916.
23. Sajoto T, Djurovich PI, Tamayo A, et al. *Inorg Chem.* 2005;44:7992.
24. Yang X, Xu X, Dang J-s, Zhou G, Ho C-L, Wong W-Y. *Inorg Chem.* 2016;55:1720.
25. Lee J, Park H, Park K-M, Kim J, Lee J-Y, Kang Y. *Dyes Pigments.* 2015;123:235.
26. Cummings SD, Eisenberg R. *J Am Chem Soc.* 1996;118:1949.
27. Li X-N, Wu Z-J, Si Z-J, Zhang H-J, Zhou L, Liu X-J. *Inorg Chem.* 2009;48:7740.